Macromolecules

Article

pubs.acs.org/Macromolecules

Water-Soluble Polymeric Photoswitching Dyads Impart Super-Resolution Lysosome Highlighters

Chong Li,[†,#] Zhe Hu,[†,#] Matthew P. Aldred,[†,§] Ling-Xi Zhao,[†] Hui Yan,[†] Guo-Feng Zhang,[†] Zhen-Li Huang,*[,†] Alexander D. Q. Li,*[,‡] and Ming-Qiang Zhu*[,†]

[†]Wuhan National Laboratory for Optoelectronics, School of Optical and Electronic Information, Huazhong University of Science and Technology, Wuhan 430074, P. R. China

[‡]Department of Chemistry, Washington State University, Pullman, Washington 99163, United States

Supporting Information

ABSTRACT: In this report, we integrated a photoswitchable quencher, a highly emissive yet pH sensitive fluorophore, and a water-soluble polymer with controlled hydrophilicity into a functional nanosystem. The photoswitching quencher is based on dithienylethene (DTE) unit, while the pH-sensitive emitter is naphthalimide (NI) unit and the water-soluble polymer is obtained from polymerization of *N*-isopropylacrylamide (NIPAM). Together, these three units create a novel super-resolution lysosome highlighter, although individually none can function as a lysotracker. Because the emitter is sensitive to pH, the resulting polymer becomes highly fluorescent in acidic lysosomes. In addition, photoswitching regulates the fluorescence on and off and thus enables super-resolution localization of fluorescent polymers with sub-40 nm spatial resolution in imaging subcellular organelles. Thus, the concept presented here, including the photoswitchable DTE-pH-sensitive NI dyad, is promising to guide the development of future-generation super-resolution imaging agents.

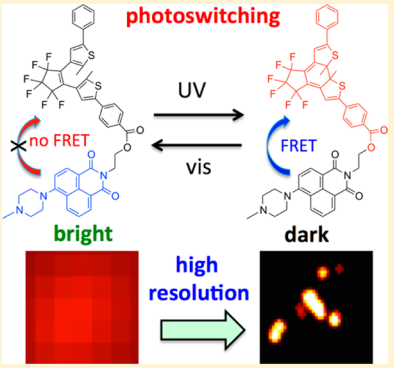

INTRODUCTION

Recently, photochromic materials and fluorescent dyes have been integrated into molecular systems to impart novel fluorescence photoswitching. The particular desired properties are good photoswitching behavior and sensory fluorescence. Dithienylethene (DTE) emerges as one of the more promising photochromic materials[1] because of its excellent fatigue resistance and thermal irreversibility.[1,2] The photochromism shuttles DTE between bistable states: one is a colorless ring-open form while the other is intensively colorful ring-closed form; this open-closed actions produce periodical energy sinks that can be used to modulate a nearby fluorophore, which can be used for fluorescent sensing and imaging in living cells.[3] Accordingly, conjugating DTE to a pH-sensitive fluorescent dye, naphthalimide (NI), produces a photoswitching molecular dyad.

One advantage of such dyads is that fluorescence photoswitching underpins super-resolution imaging based on localizing single-molecule centroid positions, thus yielding spatial resolution beyond Rayleigh's criterion.[4,5] NI-based materials have excellent photostability and high quantum yield Φ_F,[6] while DTE photoswitches efficiently with good fatigue resistance and thermal stability. Thus, covalent conjugation of DTE and NI produces a photoswitching quencher-fluorophore pair, in which Förster resonance energy transfer (FRET) can be turned on and off to modulate the emission of NI. The photoswitching dyads are easy to construct while compared with a single molecule that has both high fluorescence quantum yields (Φ_F) and desired photoswitching behavior,[7−10] because dyads split the fluorescence property and photoswitching function into two separate molecular units.

In this paper, we attached such photoswitching dyads to a water-soluble polymer whose hydrophilicity can be controlled by the transition temperature between hydrophobic and hydrophilic forms. Using the combination of photoswitching ability, pH sensitivity, and water solubility, we aim to illustrate the proof-of-principle of a new super-resolution lysosome-highlighter and here after called LysoHighlighter. Because lysosomes are widely used in cellular systems for various functions, hence the ability to monitor them is of great importance.

EXPERIMENTAL SECTION

Materials. Compound 4-bromotoluene was purchased from Energy Chemistry, while compounds 4,4′- azobis(4-cyano valeric acid) (ACVA) and 4-vinylphenylboronic acid were purchased from Sigma-Aldrich. Other commercially available starting materials, reagents, and solvents were obtained from Aladdin Chemicals and Sinopharm Chemical Reagent Co. Ltd. and used as supplied unless otherwise stated. THF was dried using sodium wires in a benzophenone system, followed by a distillation. Dimethoxyethane (DME) used in the Suzuki cross-coupling reaction was bubbled with N_2 for 30 min before usage.

Characterization. ^{1}H NMR and ^{13}C NMR spectra were recorded using a 600 M Bruker AV600 and an internal standard of

Received: July 31, 2014
Revised: November 19, 2014

 © XXXX American Chemical Society dx.doi.org/10.1021/ma501505w | *Macromolecules* XXXX, XXX, XXX−XXX

tetramethylsilane. Mass spectra were recorded using an Agilent 1100 LC/MSD Trap. Purification of intermediates and final products was accomplished mainly by gravity column chromatography, using silica gel (200−300 mesh). The UV−vis spectra were recorded using a Shimadzu UV−vis−NIR spectrophotometer (UV-3600). The PL spectra were recorded using Edinburgh instruments (FLSP920 spectrometers). The 302 nm UV irradiation for the "ring-closing" reaction was performed with an trans-illuminator (UVP, LLC, US, with four ultraviolet tubes, each 8 W 220 V; the measured power is about 0.85 mW/cm^2) and the visible light for the "ring-opening" reaction is obtained from a common household table lamp (25 W) and a long-wavelength pass filter (490 nm, accessory of the FLSP920 spectrometer). The 617 nm visible light used for chemical reaction quantum yield measurements is from a Red-Orange (617 nm) LED (LUXEON Rebel 2.28 mW cm^{-2}, Lumileds Lighting, USA). The intermediates and monomers were purified using a Waters Breeze 2 HPLC equipped with a UV detector (254 nm) and a 5-μm CN column, and HPLC-grade-eluting solvents such as DCM, EA and hexane as either pure solvents or binary mixed solvents. The molecular weight of the poly[NIPAM-*co*-(DTE-NI)] was determined by GPC using an IR detector in DMF/LiBr at 353 K. IR spectra were recorded using a Bruker VERTEX 70 spectrophotometer. The hydrodynamic diameter was measured using a dynamic light scattering instrument (ZEN3690, Malvern). The HOMO and LUMO energy levels were obtained using the B3LYP/6-31G(d) basis set.

Confocal Laser Scanning Microscopy and Super-Resolution Imaging. HeLa cells were cultured in Dublecco's modified Eagle's medium (DMEM, Invitrogen), which contained 10% fetal bovine serum (FBS) in a humidified incubator at 37 °C under 5% CO_2 atmosphere. HeLa cells were transferred into glass bottom Petri dishes grown to 80% confluence. After attachment, the cells were exposed to DMEM containing open-form poly[NIPAM-*co*-(DTE-NI)] (**1O**, 50 μg/mL), and after a 24 h exposure, the monolayer of cells was washed with PBS to remove external fluorescent dyes. Before imaging, we incubated the cells with LysoTracker Red at 75 nM for 30 min to label lysosomes. The polymer **1O** in the cells were visualized by excitation at 405 nm and fluorescence emission was collected between 510 and 540 nm using a confocal laser-scanning microscope (Olympus FluoView FV1000, Japan). Lysotracker in the cells was visualized by excitation at 561 nm, and fluorescence emission was collected between 580 and 640 nm using the same confocal laser-scanning microscope.

The optical setup for super-resolution microscopy imaging was based on a home-built system consisting of an Olympus IX 71 inverted optical microscope, a 100x/NA1.49 oil immersion TIRF objective (UAPON 100XOTIRF, Olympus), a 405 nm solid-state laser (CNILaser, China), a 302 nm UV lamp, and an EMCCD camera (Andor iXon 897). During super-resolution imaging, electronic shutters (UNIBLITZ VS14, Vincent Associates) were used to control the duration of laser irradiance and a dichroic mirror (FF509-FDi01, Semrock) and a long pass filter (BLP01−488R-25, Semrock) were used to separate the collected fluorescence from scattering laser and impurity fluorescence. We used an ImageJ plugin written in Java developed in our laboratory to analyze the image.[15] The movies were collected at a frame rate of ∼30 Hz and all durations were 2000 frames. When the 405 nm laser photoswitched on the molecular dyads and imparted fluorescence but also photobleached molecular dyads during the imaging, the weak 302 nm UV irradiation was used to regulate the emitter density by flashing on and off. We then repeated this cycle many times to collect enough data for the reconstruction of the super-resolution image.

General Synthesis. Compounds **6** (4-methylphenylboronic acid),[11] **3** (1,2-*bis*[2-bromo-5-methyl-3-thienyl]perfluorocyclopentene or Di-Br-DTE),[10] **7** (4-carboxyphenylboronic acid),[12] and **9** (2-(2-hydroxyethyl)-6-(4-methylpiperazin-1-yl)benzo[*de*]isoquinoline-1,3-dione)[13] were synthesized according to the corresponding literatures while the synthetic details of other compounds are given below.

*Compound **5**: 1-(5-Bromo-2-methyl-3-thienyl)-2-[2-methyl-5-(4-vinylphenyl)-5-thienyl]perfluorocyclopentene.* To a 100 mL two-neck round-bottom flask were added compound **3** (2.00 g, 3.80 mmol), 4-vinylphenylboronic acid (0.56 g, 3.80 mmol), Na_2CO_3 (0.81 g, 7.60 mmol), water (5 mL), and dimethoxyethane (20 mL) under N_2 atmosphere. Then the catalyst $Pd(PPh_3)_4$ (0.22 g, 0.19 mmol) was added under N_2 stream, and the reaction mixture was refluxed at 90 °C for 24 h. Water (200 mL) and ether (200 mL) were added, and the organic layer was washed with water (200 mL × 3), dried over Na_2SO_4, and concentrated under reduced pressure. The crude product was purified by gravity silica-gel column chromatography and eluted with hexane to yield a white solid (0.77 g, 36.8%). ^{1}H NMR (600 MHz, $CDCl_3$, ppm): δ = 7.52 (d, 1H, J = 8.3 Hz), 7.45 (d,, 1H, J = 8.3 Hz), 7.26 (s, 1H), 7.08 (s, 1H), 6.80−6.70 (dd, 1H, J_1 = 17.6 Hz, J_2 = 11.0 Hz), 5.81 (d, 1H, J = 17.6 Hz), 5.31 (d, 1H, J = 11.0 Hz), 1.99 (s, 1H), 1.92 (s, 2H). ^{13}C NMR (150 MHz, $CDCl_3$, ppm): δ = 143.32, 142.18, 141.29, 137.31, 136.09, 132.56, 129.32, 126.83, 125.68, 125.60, 125.51, 122.14, 114.37, 109.84, 14.57, 14.41. IR (KBr pellet): 3121−2854, 1904.4, 1809.9, 1626.1, 1548.7, 1510.7, 1470.1, 1455.2, 1439.7, 1334.2, 1269.4, 1186.3, 1113.0, 1054.9, 987.8, 902.4, 825.4, 742.8 cm^{-1}. MS (APCI, m/z): 549.3 ([M + 2]$^+$). HPLC purity: 99.5%, eluting with hexane.

*Compound **8**: 1-[(5-(4-Carboxylphenyl)-2-methyl-3-thienyl)]-2-[2-methyl-5-(4-vinylphenyl)-3-thienyl]perfluorocyclopentene.* To a 100-mL two-neck round-bottom flask were added compound **5** (0.70 g, 1.30 mmol), 4-carboxyphenylboronic acid (0.23 g, 1.40 mmol), Na_2CO_3 (0.27 g, 2.50 mmol), water (5 mL), and dimethoxyethane (10 mL) under N_2 atmosphere. Then the catalyst $Pd(PPh_3)_4$ (0.07 g, 0.064 mmol) was added under N_2 stream, and the reaction mixture was refluxed at 90 °C for 24 h. After the reation was allowed to cool down to room temperature, 0.1 M aqueous HCl (150 mL) was added. The mixture was extracted with ether (150 mL), and the organic layer was washed with water (150 mL × 3), dried over Na_2SO_4, and concentrated under reduced pressure. The crude product was purified by gravity silica-gel column chromatography and eluted with DCM: methanol (20:1) to yield a white solid (0.60 g, 50%). ^{1}H NMR (600 MHz, DMSO, ppm): δ = 13.02 (s, 1H), 7.97 (d, 2H, J = 8.4 Hz), 7.78 (d, 2H, J = 8.3 Hz), 7.68 (s, 1H), 7.62 (d, 2H, J = 8.3 Hz), 7.58−7.45 (m, 3H), 6.75 (dd, 1H, J = 17.6, 11.0 Hz), 5.88 (d, 1H, J = 17.7 Hz), 5.30 (d, 1H, J = 11.0 Hz), 2.01 (d, 6H, J = 10.8 Hz). ^{13}C NMR (151 MHz,DMSO, ppm): δ 167.27, 143.14, 141.91, 141.77, 140.93, 137.36, 136.92, 136.40, 132.38, 130.74, 130.41, 127.42, 125.93, 125.78, 125.71, 125.47, 124.69, 123.02, 115.31, 14.62, 14.57. IR (KBr pellet): 3429.7, 3081.5, 3014.6, 2919.6, 2671.9, 2546.5, 1689.0, 1607.1, 1421.1, 1318.6, 1273.8, 1193.0, 1115.0, 1055.2, 989.0, 897.2, 836.9, 774.3, 744.2, 699.2 cm^{-1}. MS (APCI, m/z): 591.2 ([M + 1]$^+$). HPLC purity: 99.0%, eluting with EA.

DTE-NI. To a mixture of compound **8** (0.20 g, 0.22 mmol), compound **9** (0.13 g, 0.22 mmol) and triphenylphosphine (0.33g, 1.26 mmol) in anhydrous THF (10 mL) at 0 °C was added dropwise a solution of diisopropyl azodicarboxylate (DIAD) (0.30 mL, 1.48 mmol) in THF (10 mL). The reaction was warmed to room temperature and stirred for 24 h. Water was added, and the product was extracted twice with dichloromethane. The combined organic layers were washed with water three times, and dried over sodium sulfate, filtered, and evaporated. The residue was chromatographed on a silica-gel column using DCM: methanol (50:1) as an eluent to yield a light yellow solid (0.20 g, 71%). ^{1}H NMR (600 MHz, $CDCl_3$, ppm): δ = 8.60 (d, 1H, J = 6.9 Hz), 8.54 (d, 1H, J = 8.0 Hz), 8.38 (d, 1H, J = 8.3 Hz), 7.98 (d, 2H, J = 8.4 Hz), 7.71 (t, 1H, J = 7.8 Hz), 7.54 (d, 2H, J = 8.4 Hz), 7.49 (d, 2H, J = 8.2 Hz), 7.42 (t, 2H, J = 6.5 Hz), 7.36 (s, 1H), 7.28 (s, 2H), 6.71 (dd, 1H J_1 = 17.6, J_2 = 10.9 Hz), 5.78 (d, 1H, J = 17.6 Hz), 5.28 (d, 1H, J = 10.9 Hz), 4.65 (s, 4H), 3.45 (s, 4H), 2.99 (s, 4H), 2.61 (s, 3H), 1.97 (d, 6H, J = 8.8 Hz). ^{13}C NMR (151 MHz, $CDCl_3$, ppm) δ = 165.97, 164.40, 163.86, 142.68, 142.08, 141.27, 141.01, 137.35, 137.26, 136.08, 132.66, 132.59, 131.39, 130.50, 129.96, 129.18, 126.81, 126.23, 126.17, 126.04, 125.78, 125.67, 125.18, 123.77, 123.23, 122.24, 114.33, 62.63, 54.67, 38.90, 29.71, 14.66, 14.61. IR (neat): 3419.4, 3075.3, 2960.3, 2925.4, 2852.1, 2744.3, 1719.5, 1698.6, 1658.6, 1589.4, 1514.0, 1456.7, 1338.5, 1270.3, 1190.5, 1111.3, 1055.0, 1019.2, 989.7, 902.3, 792.8, 760.7, 737.2 cm^{-1}. MS (APCI, m/z): 912.6 ([M + 1]$^+$). HPLC purity: 99.7%, eluting with 20% EA in DCM.

Poly[NIPAM-*co*-(DTE-NI)] (1O). DTE-NI (10 mg, 0.011 mmol), *N*-isopropylacrylamide (0.50 g, 4.42 mmol), 4,4′- azobis(4-cyano

dx.doi.org/10.1021/ma501505w | *Macromolecules* XXXX, XXX, XXX−XXX

Scheme 1. Synthetic Route to Poly[NIPAM-*co*-(DTE-NI)], a Lysosome Highlighter

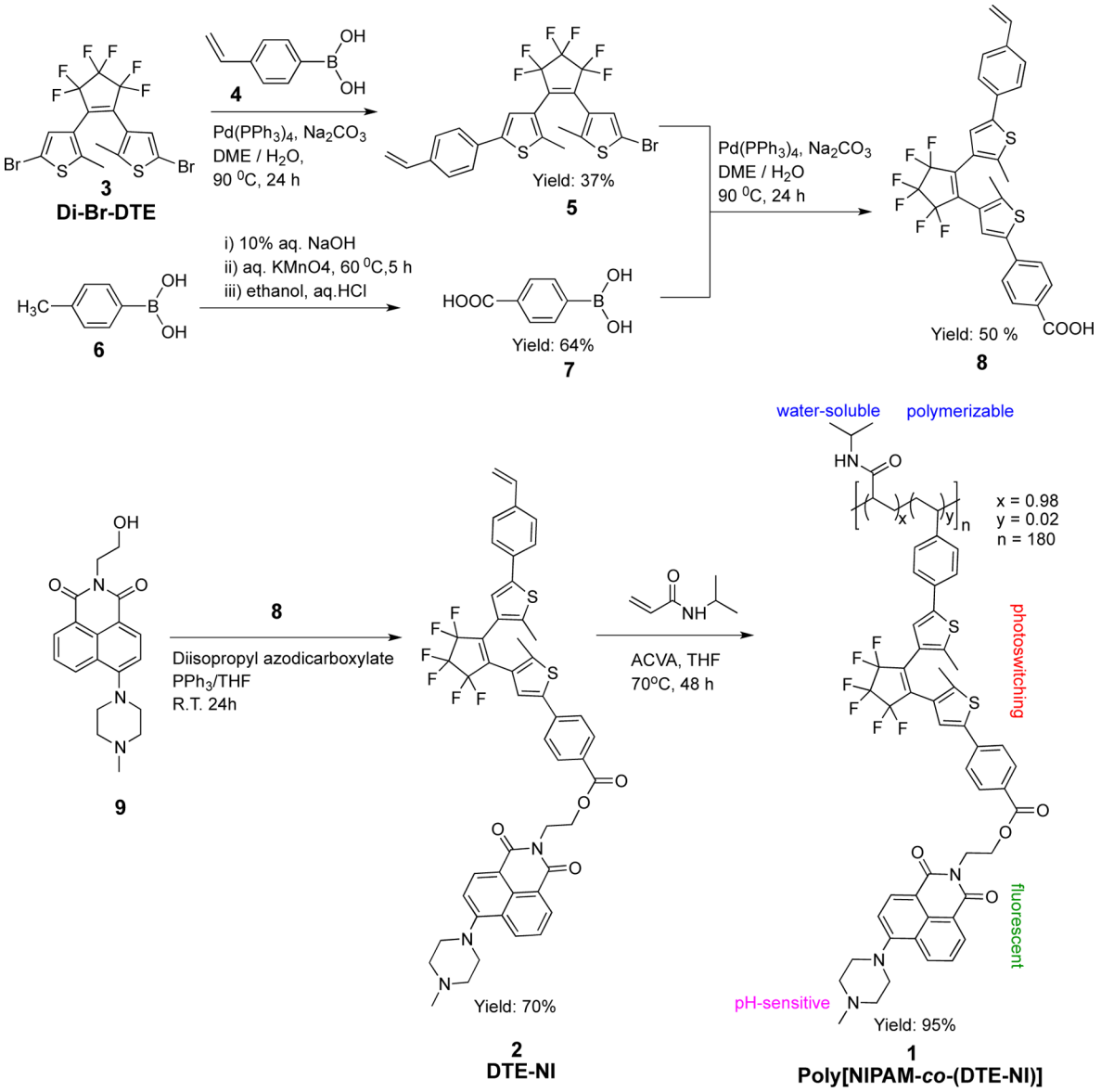

valeric acid) (ACVA, 0.01 g, 0.036 mmol), anhydrous THF (3 mL) and a small stirrer bar were added into a 10-ml dried Carius tube. The tube was subjected to three freeze−pump−thaw cycles for degasification. After the last cycle, the tube was sealed off and stirred in an oil bath at 70 °C for 48 h. After cooling down to room temperature the sealed Carius tube was opened and the resultant THF solution was dropped slowly into diethyl ether (50 mL) with constant stirring. The precipitate formed was filtered and dried under vacuum to yield a light green copolymer (0.45 g, 95%). ^{1}H NMR (600 MHz, $CDCl_3$, ppm): δ = 8.65 (d, 1H, J = 7.3 Hz, DTE-H), 8.59 (d, 1H, J = 8.0 Hz, DTE-H), 8.34 (d, 1H, J = 8.3 Hz, DTE-H), 7.99 (d, 2H, J = 8.4 Hz, DTE-H), 7.78(t, 1H, J = 7.8 Hz, DTE-H), 7.58 (d, 2H, J = 8.4 Hz, DTE-H), 7.40 (d, 2H, J = 8.2 Hz, DTE-H), 6.20 (s, 84H,PNIPAM-H), 4.68 (s, 4H), 3.93 (s, 81H, PNIPAM-H), 1.91 (m, 263H, PNIPAM-H), 1.16 (s, 458H, PNIPAM-H). ^{13}C NMR (151 MHz, $CDCl_3$, ppm): δ = 174.46 (1C), 42.49 (2C), 41.87 (1C), 22.52 (1C). IR (KBr pellet): 3438.7, 3318.3, 3073.1, 2973.3, 2935.2, 2897.5, 1651.4, 1541.8, 1459.0, 1387.1, 1367.3, 1271.0, 1234.1, 1173.1, 1130.4, 989.2, 927.5, 883.0, 838.8 cm^{-1}.

RESULTS AND DISCUSSION

Design and Synthesis of High-Resolution Lysohighlighters. The synthetic procedure for our lysohighlighter, namely poly[NIPAM-*co*-DTE-NI)], is shown in Scheme 1. Our original design used spiropyran (SP) as the photoswichable fluorescence quencher against NI. Because merocyanine (MC), the photoinduced isomer of SP, has considerable emission in the aggregated state, it was replaced by DTE. Specifically, DTE does not exhibit any fluorescence both in solution and solid state, or before and after UV-induced photoisomerization. Therefore, our design of photoswitchable molecular dyads integrates DTE with a fluorophore whose fluorescence is controlled via reversible fluorescence resonance energy transfer (FRET) to the modulated energy sink DTE. However, the fluorophore chosen is piperizine-modified naphthalimide or NI because it has pH-sensitive fluorescence, a desired feature that enables endosomes to enhance fluorescence sensitivity. The resulting photoswitchable DTE-NI dyad is covalently conjugated to a polymerizable vinyl group for LysoHighlighter construction.

dx.doi.org/10.1021/ma501505w | *Macromolecules* XXXX, XXX, XXX−XXX

Scheme 2. Acidic Lysosomes Boosting the Lysohighlighter Fluorescence Bright-to-Dark Contrast, Which Can Be Photoswitched Using External Light Sources

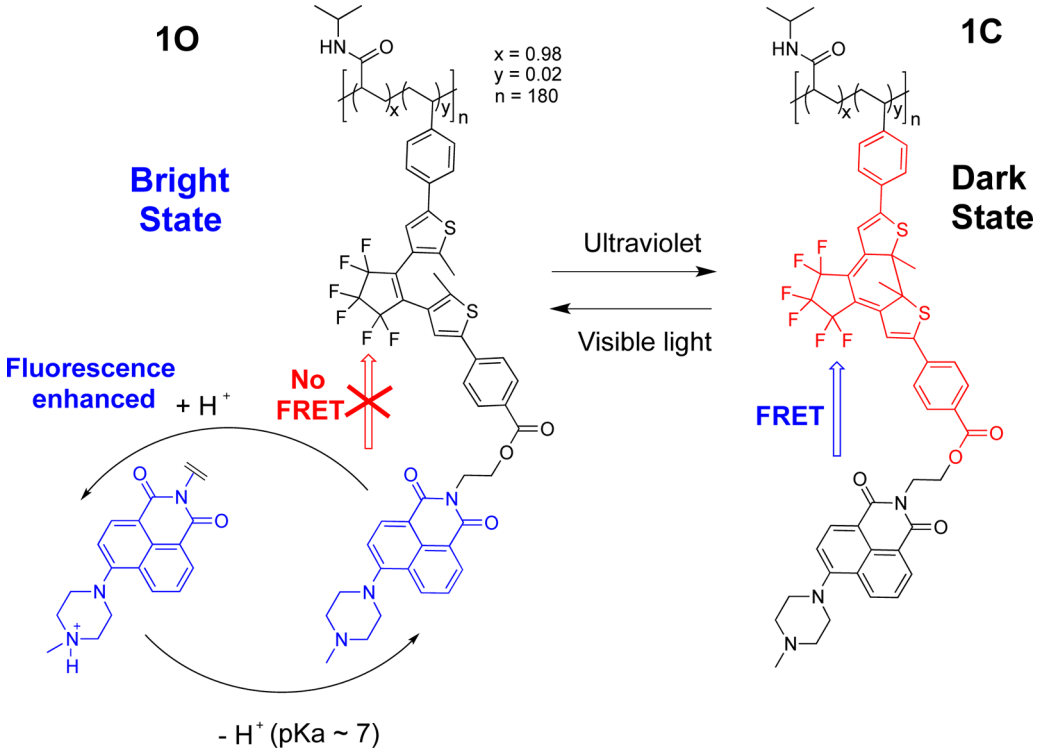

In our original design, photoswitching of spiropyran into merocyanine produces an ion pair of a positive and a negative charge, which gain hydrophilic features for the molecular photoswitch. Compared with spiropyran−merocyanine system, DTE is always hydrophobic including the open form before UV-irradiation and the closed form after UV-irradiation. However, hydrophobic DTEs exhibit great photoswitching reversibility in both organic and aqueous solutions. To address the issue of lacking hydrophilicity, the pH-sensitive, photoswitchable, fluorescent dyad (DTE-NI) is integrated with a water-soluble monomer, NIPAM. Consequently, the resulting water-soluble polymer, poly[NIPAM-*co*-(DTE-NI)], has salient features as detailed below: (1) its pH-sensitive fluorescence is tremendously enhanced in acidic microenvironment such as lysosomes; (2) the enhanced fluorescence can be photoswitched on and off using visible and UV light, respectively; (3) its hydrophilicity and hydrophobicity can be regulated by the environmental temperature suitable for biosensing and bioimaging.

Accordingly, the syntheses were carried out to manifest the predesigned procedure. The scaffold of the photoswitchable quencher, 1-(5-bromo-2-methyl-3-thienyl)-2-[2-methyl-5-(4-vinylphenyl)-5-thienyl]perfluorocyclopentene (**5**) was synthesized using Suzuki cross-coupling reaction between dibromo-DTE and 4-vinylphenylboronic acid with 36% yield followed by further Suzuki cross-coupling reaction with 4-carboxyphenylboronic acid to afford monomer **8** with 50% yield. Fluorescent monomer DTE-NI was prepared by etherization between **8** and **9** with 71% yield. The solubility of DTE-NI is great in common organic solvents, but DTE-NI cannot be dissolved in water even though it is sensitive to pH changes. Therefore, DTE-NI was copolymerized with a hydrophilic monomer *N*-isopropylacrylamide (NIPAM) to yield a water-soluble and pH-sensitive polymer poly[NIPAM-*co*-(DTE-NI)].

Integrating the monomeric dyads into poly(*N*-isopropylacrylamide) or PNIPAM side-chains gains aqueous solubility for molecular photoswitches, which offer more flexibility in biocompatible and bioconjugate modifications. The gel permeation chromatography (GPC) measurements yield the mean molecular weight of 24 000 Da with a molecular weight distribution index of 1.92 (Figure S1, Supporting Information). At 25 °C, the photoswitchable polymer is quite water-soluble and has no detectable light scattering, indicating that it exists as free macromolecules in water. At 37 °C and above the lower critical solution temperature (LCST), however, the same photoswitchable polymer becomes rather hydrophobic and in aqueous solution it begins to aggregate into large nanoparticles (∼115 nm), which can be measured using dynamic light scattering (Figure S2).

Photophysical and Photochemical Properties. The new LysoHighlighter, capable of super-resolution (vide infra), are both photoresponsive and pH-sensitive as illustrated in Scheme 2. Absorption spectra of polymer **1** are depicted in Figure 1a, which shows that the open form **1O** has an intense absorption band at 318 nm and ∼400 nm due to DTE subunit and NI subunit, respectively (Figure S4), whereas the closed form **1C** has a characteristic and photoswitchable band at 600 nm with a molar extinction coefficient ∼1.8 × 10^4 M^{-1} cm^{-1}. Conversely, the molar extinction coefficients of open form are 5 × 10^4 M^{-1} cm^{-1}at 318 nm (DTE) and 1 × 10^4 M^{-1} cm^{-1} at 400 nm (NI). Upon 302 nm UV-light irradiation, the photoswitchable band grows, corresponding photochemical conversion from **1O** to **1C** with a cyclization yield of 98% (Figure S3). Conversely, visible light causes the photoswitchable band to decrease in intensity due to the back-conversion from **1C** to **1O**. Thus, polymer **1** has the desired bistable photochromism and can be reversibly photoswitched between those two states for many cycles (Figure 1b). The

dx.doi.org/10.1021/ma501505w | *Macromolecules* XXXX, XXX, XXX−XXX

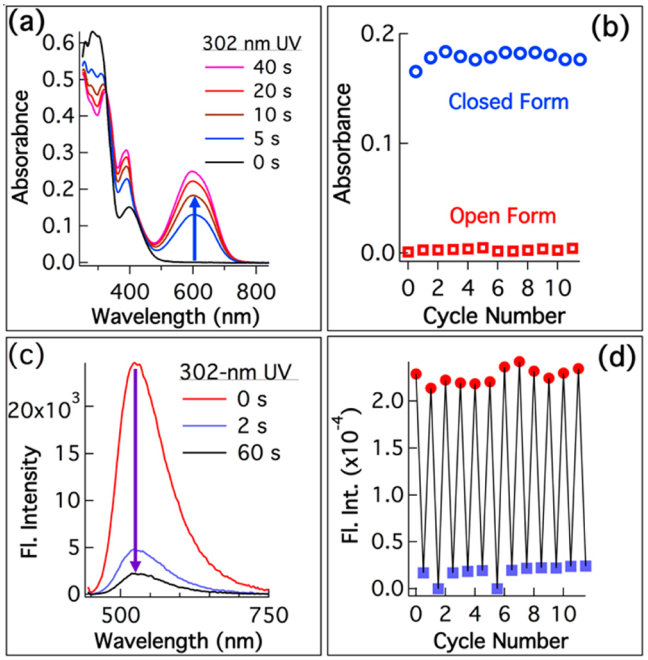

Figure 1. (a) The open form polymer **1O** has intense bands at 318 and 400 nm due to optical absorption from DTE and NI subunits, respectively. When polymer **1O** is irradiated with 302 nm UV light, the photochromic band at 600 nm ($\varepsilon = 1.8 \times 10^4$ M^{-1} cm^{-1}) emerges and grows as more **1O** is converted to **1C** and (b) this interconversion can be switched for more than 10 cycles reversibly. (c) Upon 302 nm irradiation, the emission intensity collapses as the molecule changes from the bright state (**1O**) to the dark state (**1C**). (d) Fluorescence intensity (monitored at 524 nm) oscillates between maximum and minimum, as photoswitching is alternating between 302 nm irradiation (20 s) and ≥490 nm (5 min) illumination. The concentration of **1** is 1 mg/mL in water and the fluorescence excitation wavelength is 440 nm.

photochromic properties of polymer **1** come from the DTE-NI dyad. The cyclization quantum yield and its reversal ring-opening quantum yield for the **DTE-NI** dyad are 0.46 under UV and 0.007 under 617 nm irradiation, respectively; these values are measured from the photokinetics curves in Figure S5 using methods previously reported.[14] Polymer **1O** hence exhibits green fluorescence, whose intensity can be turned off by UV radiation and recovered by visible light.

Because photochromism and fluorescence are separated into two subunits in the dyad, thus photochromism is accompanying with fluorescence photoswitching. The open form **1O** emits strongly at 524 nm with a large Stokes shift (114 nm), whose origin can be assigned to the NI unit. Upon 302 nm irradiation, the fluorescence intensity of the 524 nm band plummeted dramatically because irradiation converted the nonquenching open-form DTE to the quenching closed-form counterpart (Figure 1c). The close proximity between ring-closed DTE and NI contributes to the efficient resonance energy transfer. The second factor that contributes to efficient resonance energy transfer is the large spectral overlap integral between fluorescent NI donor and the ring-closed DTE quencher because NI emits from 470 to 650 nm and DTE absorbs from 500 to 700 nm (Figure S4b).[5,9,15] Förster distance calculated based on the spectral overlap integral is 6.4 nm, which ensures nearly 100% FRET efficiency between the ring-closed DTE quencher and the NI donor. The efficient FRET quenching mechanism produces the dark state (**1C**). When the visible light switches the DTE into the ring-open form, there is no spectral overlap between the ring-open DTE and the NI dye. Hence the fluorescence intensity of NI is not quenched, yielding the bright state for the polymeric system (**1O**). The fact that fluorescence intensity depends on the overlap integral only indicates that fluorescence quenching mechanism is energy transfer.

Because FRET is at 100% efficiency in this system and can occur over a longer distance, other quenching mechanisms that require close contact including photoinduced electron transfer (PET) cannot effectively compete with FRET quenching mechanisms.[16] The simple reason is that FRET mechanism already quenches the donor excitation energy before the NI and DTE subunits reach each other. In the photoswitchable bright and dark system of **1O** and **1C**, the excellent photostability of NI, the remarkable fatigue resistance of DTE, and the relatively high cyclization quantum yield (0.46) produce great reversibility of the photoswichable fluorescence.

The reversibility of fluorescence photoswitching was demonstrated using alternating UV and visible light irradiations, which cycled the forward and backward photochemical reactions between **1O** and **1C**. Pure **1O** established the maximum fluorescence intensity in aqueous solutions when excited at 440 nm. After 302 nm UV-light irradiation, the strong emission intensity at 524 nm dropped more than 90% due to photoswitched dyad quenching. This cycling behavior under alternating UV and visible light irradiation exhibits decent reversibility and good fatigue resistance (Figure 1d). Similarly, monomer DTE-NI in THF mimics the same photochromic behavior and fluorescence photoswitching (Figure S6). Therefore, polymer **1O** in neutral pH aqueous solutions possesses higher than 10 times fluorescence bright-to-dark contrast ratio, an attractive feature for super-resolution or frequency-domain fluorescence imaging.[17]

Interestingly, piperazine has two pK_a values: the first pK_{a1} is estimated to 2−3 and the second pK_{a2} is ∼7.[15a] The protonation and deprotonation of the piperazine subunits in the NI unit enable pH sensitivity of fluorescence (Scheme S2), while the NIPAM subunits impart thermal sensitivity. As a result fluorescence intensity of polymer **1O** in aqueous solution is sensitive to both pH and temperature changes. For instance, fluorescence intensity was doubled when temperature rose from 20 to 40 °C (Figure S7), because lower critical solution temperature (LCST) caused a phase transition from a swollen hydrated state to a dense dehydrated state. Similarly, fluorescence quantum yield, Φ_F of polymer **1O**, increased by 5-fold (3% → 15%) when pH changed from 8.3 (non-protonated piperazine) to 2.7 (protonated piperazine) (Figure S8 and Table S1). The likely reason is that piperazine group quenches NI fluorescence via photoinduced electron transfer (PET) because the imide on the NI unit is a good electron acceptor and the amino group on the piperazine is a good electron donor. When the piperazine is protonated, the amino group loses its ability to donate electron and 12% recovered quantum yield was obtained. As a rule of thumb, lower pH and shorter irradiation wavelength not only increase photoswitching rates but also boost fluorescence bright-to-dark contrast ratios to as high as 110 times (Figure S9 and Figure S10), enhancing photoswitching fluorescence imaging in acidic lysosomes.

The tertiary amino group on NI is far from the photochromic DTE, the probability of electron transfer between them would be very low or negligible. Similarly, the imide group on NI is not closed enough to the DTE to efficiently trigger PET because those two components are separated by a flexible chain

dx.doi.org/10.1021/ma501505w | *Macromolecules* XXXX, XXX, XXX−XXX

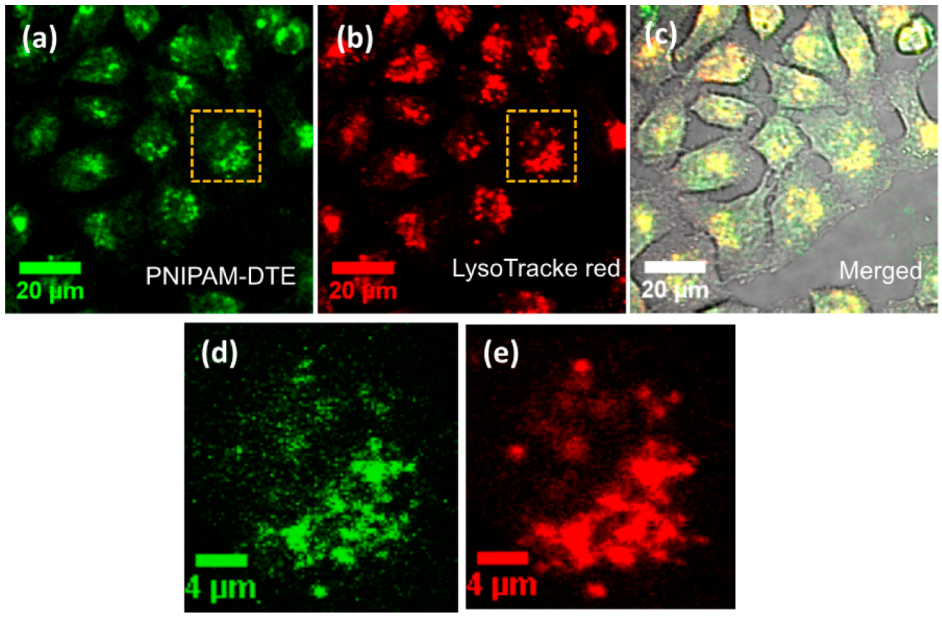

Figure 2. Confocal laser scanning microscope (CLSM) images of living HeLa cells incubated with polymer **1O** (50 μg/mL) and LysoTracker Red (75 nM). (a) The image of polymer **1O** (λ_{ex} = 405 nm), (b) image of LysoTracker Red (λ_{ex} = 561 nm). (c) The green-fluorescence and red-fluorescence images in parts a and b are merged with the bright-field image. (d and e): Zoomed-in views identified by the boxes in parts a and b reveal that lysohighlighter and lysotracker have essentially the same patterns.

(−CO−O−CH_2−CH_2−). Actually, the tertiary amino group shows strong electron transfer with NI-imide core, resulting in low fluorescence quantum yield in the nonprotonated state as discussed above. Shown in Figure S12, the open-form DTE displays a higher LUMO but a lower HOMO than those of NI. The PET process might possibly happen during the photoswitching process, but not the fluorescence excitation. For the closed form DTE-NI, the excited state of the DTE would not be able to activate PET from NI owing to mismatched energy levels.

The water-solubility of polymer **1** provides a novel platform for bioimaging in physiological conditions. Human epithelial cervical cancer cell or HeLa cells were stained with both LysoTracker Red (75 nM) and polymer **1** in PBS buffer (pH = 7). MTT assay confirmed that polymer **1** was not cytotoxic to the cells at 20−500 μg/mL level (Figure S11) because cellular viabilities were estimated to be ∼100% within 48 h. Confocal microscopy reveals the colocalization of polymer **1** (green fluorescence) with commercial LysoTracker Red, confirming that polymer **1** has high cell permeability and is selectively accumulated in the acidic organelles (Figure 2). In lysosomes (pH = 4.5−5.0), the lower pH pushes protonation on polymer **1** and thus enhances green-fluorescence, resulting in the localization of several small lysosomes emitting green fluorescence in the cytoplasm.[15] The Pearson's correlation coefficient[18] between the green emissions from polymer **1** (Figure 2a and 2d) and the red emissions (Figure 2b and 2e) from LysoTracker Red was determined to be 86.8%, indicative a nearly perfect correlation. Therefore, polymer **1** functions as a new lysohighlighter green.

Lysohighlighters Impart Super-Resolution Imaging. The above green fluorescence highlighting of HeLa cells can be turned on and off. For example, the 405 nm near-UV irradiation cannot switch **1O** to **1C**, yet excites strong green fluorescence. A higher energetic photon (<365 nm) can switch off the green fluorescence, e.g., 302 nm UV light at 0.40 mW/cm^2 for 10 s. It is moteworthy that even 1-s 405 nm excitation swiftly switches the green fluorescence back on (Figure S12).

The ability to switch fluorescence *on* and *off* provided the opportunity for observing many subcellular structures beyond the diffraction limit in super-resolution imaging.[19,20] The fluorescence *on* and *off* can be imparted with 405 nm laser (∼10 mW/cm^2) and 302 nm UV light (∼0.40 mW/cm^2) (Figure S12), respectively. The 405 nm light only excites the fluorophore that emits at 524 nm, whereas the 302 nm light causes cyclization of the DTE moiety in polymer **1** and switches off the fluorescence. Accordingly, HeLa cells were cultivated with polymer **1** for super-resolution imaging using a home-built microscope and algorithm.[21]

Because the polymer preferred to reside in lysosomes, small spherical lysosomes in the treated cells emitted strong fluorescence under acidic conditions (Figure 3, parts a and b). Evidently, fluorescent clusters crowded within the lysosome, most fluorescent points are so close that individual fluorophores cannot be clearly distinguished using conventional fluorescence imaging techniques (Figure 3, parts c and d). Super-resolution images, however, clearly demonstrate nanoscale localization of separated fluorescent points in Figure 3, parts e and f, corresponding to DTE-NI molecular dyads. In super-resolution images, each bright spot emerged from repeated localizations of individual photoswitchable DTE-NI pairs over multiple photoswitching cycles. For example, two fluorescent points separated by 40 nm apart can be well differentiated in the super-resolution image (Figure 3, parts f and g).

Although the closely related two-point resolution can be calculated using the number of photon detected,[22] the overall resolution of a diffraction-unlimited image is recently described using the Fourier ring correlation (FRC).[19] As an integral and practical resolution measure, FRC was used to determine the resolution in optical nanoscopy and yielded a calculated resolution of 42.9 ± 0.6 nm (Figure S13). The fwhm (full width at half-maximum) of the localized polymer probes are

dx.doi.org/10.1021/ma501505w | *Macromolecules* XXXX, XXX, XXX−XXX

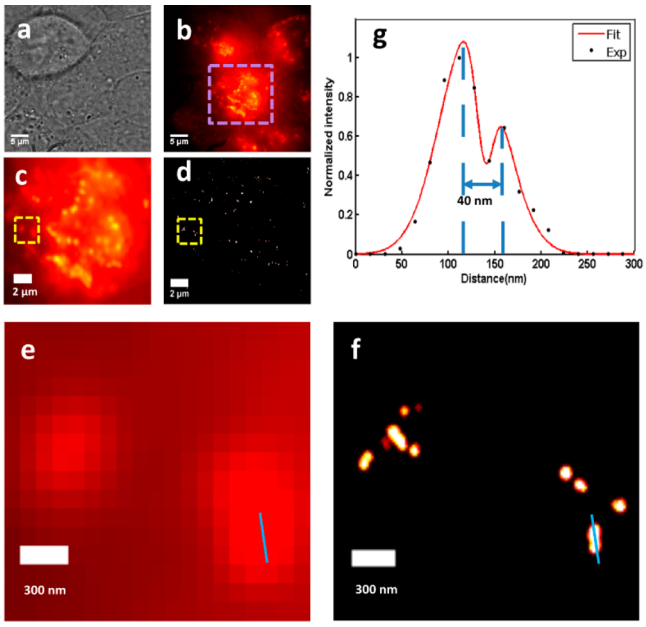

Figure 3. Polymer **1** was used in super-resolution imaging to label lysosomes of HeLa cells. (a) Bright field image. (b) Conventional fluorescence image displaying the distribution of polymer **1**. (c) Expanded view of the conventional fluorescence image marked by the purple box in part b. (d) Super-resolution image of the same purple box marked in part b. Images e and f are enlarged views of the yellow boxes marked in parts c and d, respectively, revealing the dramatic enhancement of the super-resolution technique. (g) Fluorescence cross-sectional profiles of a pair of vicinal fluorescent points along the dashed lines in part f, indicating that structures of 40 nm apart have been resolved.

determined to be 35 nm using Gaussian deconvolution (Figure S14). The fwhm gives a standard deviation of 15 nm, indicating a resolution around 40 nm, which agrees with the FRC method. The most recent research reported that the average position precision of fluorescent molecular labels could even be below 1 nm regardless of the size of labels.[23] At such resolutions, fluorescence super-resolution imaging is comparable to electron microscopy.

CONCLUSIONS

In conclusion, we have designed and synthesized a novel photoswitchable fluorescent polymer that contains a pH-sensitive and photoswitchable molecular dyad DTE-NI. Copolymerization with NIPAM resulted in a water-soluble polymer whose hydrophilicity can be controlled via temperature. Such a polymer **1** with integrated functions exhibits reversible fluorescence *on-and-off* photoswitching properties in aqueous solutions when alternating irradiation of visible and UV light is applied. Amazingly, pH-sensitive fluorescence makes polymer **1** a new lysohighlighter because its fluorescence is significantly enhanced in acidic microstructures like lysosomes in cellular imaging. Photoswitching-based super-resolution fluorescence imaging demonstrates that such lysohighlighters are capable of resolving 40 nm subcellular structures, much higher than conventional fluorescence imaging using traditional lysotracker. Thus, photoswitchable fluorescent polymers with multifunctions integrated into a macromolecule are promising next-generation imaging agents for super-resolution bioimaging.

ASSOCIATED CONTENT

Supporting Information

GPC curves of **1O**, dynamic light scattering of **1O**, cyclization reaction yields calculation, optical properties of DTE-NI and **1O**, 5. MTT assay, fluorescence switching imaging, super-resolution microscopy imaging, DFT calculation, NMR spectra, mass spectra, and IR spectra. This material is available free of charge via the Internet at http://pubs.acs.org.

AUTHOR INFORMATION

Corresponding Authors

*(M.-Q.Z.) E-mail: mqzhu@hust.edu.cn.
*(Z.-H.L.) E-mail: leo@mail.hust.edu.cn.
*(A.D.Q.L.) E-mail: dequan@wsu.edu.

Present Address

[§]Department of Chemistry, Durham University, South Road, Durham DH1 3LE, U.K.

Author Contributions

[#]These authors contributed equally.

Notes

The authors declare no competing financial interest.

ACKNOWLEDGMENTS

This work was supported by the National Basic Research Program (973) of China (2015CB755602 and 2013CB922104), the National Science Foundation of China (NSFC 21474034 and 21174045), and the National Science Foundation (CHE-1213358). M.P.A. is the Foreign Young Investigator Awardee of NSFC (21150110141 and 212111128). Z.-L.H acknowledges financial support from the Program for New Century Excellent Talents in University of China (Grant No. NCET-10-0407). We also thank the Analytical and Testing Center of Huazhong University of Science and Technology and the Center of Micro-Fabrication and Characterization (CMFC) of WNLO for use of their facilities.

REFERENCES

(1) Irie, M. *Chem. Rev.* **2000**, *100*, 1685−1716.
(2) (a) Tian, H.; Yang, S. *Chem. Soc. Rev.* **2004**, *33*, 85−97. (b) Guo, X. F.; Zhang, D.; Gui, Y.; Wax, M. X.; Li, J. C.; Liu, Y. Q.; Zhu, D. B. *Adv. Mater.* **2004**, *16*, 636−640. (c) Yun, C.; You, J.; Kim, J.; Huh, J.; Kim, E. *J. Photochem. Photobiol. C: Photochem. Rev.* **2009**, *10*, 111−129.
(3) Matsuda, K.; Irie, M. J. *Photochem. Photobiol. C: Photochem. Rev.* **2004**, *5*, 169−182.
(4) (a) Heilemann, M.; Dedecker, P.; Hofkens, J.; Sauer, M. *Laser Photonics Rev.* **2009**, *3*, 180−202. (b) Tian, Z.; Wu, W.; Li, A. D. Q. *ChemPhysChem* **2009**, *10*, 2577−2591.
(5) (a) Li, C.; Gong, W.-L.; Hu, Z.; Aldred, M. P.; Zhang, G.-F.; Huang, Z.-L.; Zhu, M.-Q. *RSC Adv.* **2013**, *3*, 8967−8972. (b) Zhu, M.-Q.; Zhang, G.-F.; Hu, Z.; Aldred, M. P.; Li, C.; Gong, W.-L.; Chen, T.; Huang, Z.-L.; Liu, S. *Macromolecules* **2014**, *47*, 1543−1552.
(6) (a) Tian, H.; Gana, J.; Chena, K.; He, J.; Song, Q. L.; Hou, X. Y. *J. Mater. Chem.* **2002**, *12*, 1262−1267. (b) McAdam, C. J.; Robinson, B. H.; Simpson, J. *Organometallics* **2000**, *19*, 3644−3653.
(7) (a) Irie, M.; Fukaminato, T.; Sasaki, T.; Tamai, N.; Kawai, T. *Nature* **2002**, *420*, 759−760. (b) Zhou, Z.; Hu, H.; Yang, H.; Yi, T.; Huang, K.; Yu, M.; Li, F.; Huang, C. *Chem. Commun.* **2008**, 4786−4788. (c) He, Y.; Zhu, Y.; Chen, Z.; He, W.; Wang, X. *Chem. Commun.* **2013**, *49*, 5556−5558.
(8) (a) Zhu, M.-Q.; Zhang, G.-F.; Li, C.; Aldred, M. P.; Chang, E.; Drezek, R. A.; Li, A. D. Q. *J. Am. Chem. Soc.* **2011**, *133*, 365−372. (b) Zhu, M.-Q.; Zhang, G.-F.; Li, C.; Aldred, M. P.; Li, A. D. Q. *J. Innovative Opt. Health Sci.* **2011**, *4*, 395−408.

(9) Gong, W.-L.; Zhang, G.-F.; Li, C.; Aldred, M. P.; Zhu, M.-Q. *RSC Adv.* **2013**, *3*, 9167−9170.
(10) Li, C.; Yan, H.; Zhang, G.-F.; Gong, W.-L.; Chen, T.; Hu, R.; Aldred, M. P.; Zhu, M.-Q. *Chem.—Asian J.* **2014**, *9*, 104−109.
(11) Qu, D. H.; Wang, G. C.; Ren, J.; Tian, H. *Org. Lett.* **2004**, *6*, 2085−2088.
(12) Ma, S.; Sun, D.; Forster, P. M.; Yuan, D.; Zhuang, W.; Chen, Y.-S.; Parise, J. B.; Zhou, H.-C. *Inorg. Chem.* **2009**, *48*, 4616−4618.
(13) Tian, H.; Gana, J.; Chena, K.; He, J.; Song, Q. L.; Hou, X. Y. *J. Mater. Chem.* **2002**, *12*, 1262−1267.
(14) (a) Gillanders, F.; Giordano, L.; Díaz, S. A.; Jovin, T. M.; Jares-Erijman, E. A. *Photochem. Photobiol. Sci.* **2014**, *13*, 603−612. (b) Giordano, L.; Jovin, T. M.; Irie, M.; Jares-Erijman, E. A. *J. Am. Chem. Soc.* **2002**, *124*, 7481−7489.
(15) (a) Tian, Y.; Su, F.; Weber, W.; Nandakumar, V.; Shumway, B. R.; Jin, Y.; Zhou, X.; Holl, M. R.; Johnson, R. H.; Meldrum, D. R. *Biomaterials* **2010**, *31*, 7411−7422. (b) Giordano, L.; Jovin, T. M.; Irie, M.; Jares-Erijman, E. A. *J. Am. Chem. Soc.* **2002**, *124*, 7481−7489.
(16) Zhao, H.; Al-Atar, U.; Pace, T. C. S.; Bohne, C.; Branda, N. R. *J. Photochem. Photobiol. A* **2008**, *200*, 74−82.
(17) (a) Hu, D.; Tian, Z.; Wu, W.; Wan, W.; Li, A. D. Q. *J. Am. Chem. Soc.* **2008**, *130*, 15279−15281. (b) Li, A. D. Q.; Zhan, C.; Hu, D.; Wan, W.; Yao, J. *J. Am. Chem. Soc.* **2011**, *133*, 7628−7631.
(18) Gota, C.; Okabe, K.; Funatsu, T.; Harada, Y.; Uchiyama, S. *J. Am. Chem. Soc.* **2009**, *131*, 2766−2767.
(19) Nieuwenhuizen, R. P. J.; Lidke, K. A.; Bates, M.; Puig, D. L.; Grünwald, D.; Stallinga, S.; Rieger, B. *Nat. Methods* **2013**, *10*, 557−562.
(20) Durisic, N.; Laparra-Cuervo, L.; Sandoval-Álvarez, Á.; Borbely, J. S.; Lakadamyali, M. *Nat. Methods* **2014**, *11*, 156−162.
(21) Quan, T.; Li, P.; Long, F.; Zeng, S.; Luo, Q.; Hedde, P. N.; Nienhaus, G. U.; Huang, Z.- L. *Opt. Express* **2010**, *18*, 11867−11876.
(22) Ram, S.; Ward, E. S.; Ober, R. J. *Proc. Natl. Acad. Sci. U.S.A.* **2006**, *103*, 4457−4462.
(23) Szymborska, A.; de Marco, A.; Daigle, N.; Cordes, V. C.; Briggs, J. A. G.; Ellenberg, J. *Science* **2013**, *341*, 655−658.